

Cite this: *RSC Sustainability*, 2026, 4, 262

Sustainable synthesis of hydroxyapatite-containing composites from eggshells for soil amendment applications

Letizia Castellini, Alessia Giordana, * Mery Malandrino, Lorenza Operti and Giuseppina Cerrato *

Managing large volumes of food waste is a growing challenge. Eggshells (ESs) are an abundant and widespread waste that represent an interesting source for Ca-based materials. To fulfil the cradle-to-cradle sustainability concept, the final products need to be materials that can either degrade or serve as nutrients in soil. ES can be converted into different Ca precursors to obtain hydroxyapatite (Hap) nanoparticles, a promising solid fertilizer that can promote a controlled release of nutrients. Most of the reported procedures involve a high-temperature calcination step to obtain CaO, a process that is energy-intensive and CO₂ emitting. We propose an alternative by dissolving ES in an ascorbic acid solution, a green, non-toxic, and cost-effective reagent. Composition, crystallinity and morphology of the obtained product were compared to those of Hap obtained with commercial reagents and by dissolving ES in nitric acid. Nutrient release behaviour was evaluated through ICP-OES, demonstrating the material's potential for agricultural applications. This method offers a low-impact, circular approach to waste valorisation, promoting the conversion of food waste into high-value functional materials.

Received 9th July 2025
Accepted 14th November 2025

DOI: 10.1039/d5su00577a

rsc.li/rscsus

Sustainability spotlight

This study deals with a sustainable route for the synthesis of hydroxyapatite *via* a low-temperature aqueous method using calcium-rich eggshell waste and ascorbic acid as a green reagent. By means of this process, the need for high-temperature calcination can be avoided, significantly reducing the energy input. The obtained hydroxyapatite is tailored for application as a slow-release fertilizer, enhancing phosphorus bioavailability while minimizing nutrient leaching. This biowaste valorisation aligns with the principles of both green chemistry and circular economy, directly supporting the following UN Sustainable Development Goals: SDG 12 (Responsible Consumption and Production), SDG 2 (Zero Hunger), SDG 13 (Climate Action) and SDG 14 (Life Below Water) by promoting resource efficiency, sustainable agriculture, and reduced carbon footprint.

Introduction

The management of large amounts of food waste presents a significant challenge. Circular economy aims at minimizing waste and promotes continuous reuse of materials as resources to produce value-added products, addressing sustainability and pollution concerns.¹ Eggshells (ESs) are a common and widespread waste. In 2023, world eggs production reached 97 million tons, a 40% increase compared to 2010. In the past 30 years, world eggs production has increased by 150% with the most remarkable growth observed in Asia. Asia was the main producer of hen eggs in 2023, accounting for 64% of the global production, followed by the Americas (20%), Europe (12%), Africa (4%) and Oceania (0.4%).² ES has been ranked as the 15th major food industry pollution problem by the Environmental Protection Agency and is considered as hazardous waste

(category 3) in the European Union.³ ES accounts for approximately 11% of an egg's weight, resulting in 7.2 million tons of ES waste produced annually: this waste is typically disposed of in landfills, where it generates unpleasant odours and promotes microbial growth.⁴ ES is composed of calcium carbonate (~94%), calcium phosphate (~1%), magnesium carbonate (~1%) and organic matter (~4%) and can be converted into different Ca precursors.⁵ Recovering ES waste to produce high-value goods is a valuable recycling strategy. A range of possible applications has been proposed, such as the use of ES-derived materials for the removal of toxic metals from contaminated water and soil,^{6–9} the substitution of lime in cement production,¹⁰ the production of polymer¹¹ and metal composites and the synthesis of biomaterials as hydroxyapatite (Hap).⁴ Most of the literature studies involve a preliminary thermal treatment ($T \geq 700$ °C) to convert ES into CaO.^{12,13} This step is highly energy-intensive and generates a significant amount of CO₂ due to the decomposition of calcium carbonate. A recent life cycle assessment study indicates that the calcination step is

Department of Chemistry, Università Degli Studi di Torino, Via Pietro Giuria 7, 10125 Turin, Italy. E-mail: alessia.giordana@unito.it; giuseppina.cerrato@unito.it



To synthesize 0.001 mol of Hap using ES, 0.01 mol of CaCO_3 (1 g of ES powder) and 0.006 mol of H_3PO_4 were used. Hap-2 was synthesized after dissolving ES in HNO_3 solution (20 ml, 0.02 mol). The solution was magnetically stirred until ES powder was fully dissolved (150 min). Hap-3 was synthesized after dissolving ES powder in HAsc solution. HAsc (0.03 mol) was dissolved in 40 ml of water, and ES powder was gradually added, enhancing CO_2 capture with subsequent production of oxalate ions (according to the general reaction scheme reported in the SI). The solution was magnetically stirred until ES powder was fully dissolved (4 h). The next steps were conducted identically for both samples. The resulting solutions were basified to pH = 11 by adding a 2 M KOH solution (~20 ml). Subsequently, H_3PO_4 , diluted in 20 ml of distilled water, was added dropwise under continuous stirring. During the reaction, the pH was controlled and maintained above 10.5 by addition of ammonia solution, if necessary. The suspension was stirred for a further 2 h and then allowed to stand overnight. The final product was filtered under suction and dried in air.

The overall yield in weight is 0.98 g for Hap-2, and 1.90 g for Hap-3. In the latter case, it is not possible to calculate % yield due to the co-presence of calcium oxalate and other organic residues in the final product.

An overview of the synthesized samples is provided in Table 1.

GCM approach

The GCM approach was applied to each of the synthesized samples (Hap-1, Hap-2, and Hap-3) and to a literature product,²⁸ obtained through the wet-precipitation method and involving the calcination step (indicated as Hap-4 in Table 1). Principle-specific scores were determined, following the equations reported by DeVierno Kreuder *et al.*²⁵ These scores were used to determine the category rank for the three categories: improved resource use (principles 1-2-7-8-9-11), increased energy efficiency (principle 6), and reduced human and environmental hazard (principles 3-4-5-10-12). A lower category rank indicates a greener process.

Ion release study

To evaluate the release of ions from the matrix, 0.21 g of each sample were suspended in 10 ml of D. I. water. Every 24 h, the solid was separated by centrifugation (8000 rpm, 5 min) and the same volume of fresh water was re-added. The released Ca, K, and P ions were quantified by inductively coupled plasma optical emission spectroscopy (ICP-OES).

Results and discussion

Data of characterization techniques (as discussed below) indicate that Hap-based materials can be successfully obtained using ES powder as the Ca source. The proposed synthetic procedure, that avoids any thermal treatment, involved at first the dissolution of ES powder in an acid solution (HNO_3 or HAsc). Then the solution was basified using KOH and Hap was obtained *via* wet precipitation using H_3PO_4 . Some differences can be noted in the synthesis according to the employed acid. In fact, when ES powder is dissolved in HNO_3 solution, the production of both bubbles and foam was observed due to a strong CO_2 release. Part of the released gas formed carbonate ions that partially substitute phosphate ions in the lattice of the final product: in fact, c-Hap is obtained. On the other hand, dissolution in HAsc solution generates a minimal amount of bubbles and foam, thanks to the formation of oxalate ions. This represents an advantage in terms of the scalability of the process. Due to the low solubility of Ca oxalate, this co-product starts to precipitate before Hap and so could be possibly separated. Various experimental trials were conducted to optimize the synthesis conditions, in particular to minimize the quantity of employed acid and dissolution time. Multiple syntheses were performed for Hap-2 and Hap-3, and reproducible results in terms of the obtained product and yield were obtained.

The results of PXRD, reported in Fig. S1–S3, indicate the formation of crystalline products. The analyses of the diffractogram of Hap-3 indicate the formation of Hap (ICDD-PDF 01-084-1998) and the co-presence of two crystalline forms of calcium oxalate (CaOx). In detail, the peaks at 14.3, 32.2 and 20.1° are attributable to dihydrate CaOx (weddellite, ICDD-PDF 00-017-0541), while signals at 14.9, 24.4 and 30.1° indicate the formation of the monohydrate phase (whewellite, ICDD-PDF 00-014-0769). If compared to Hap-1, Hap-3 exhibits a reduced crystallinity of the Hap phase and a reduced dimension of the crystallite. In turn, Hap-2 exhibits a pattern consistent with the formation of carbonated-substituted Hap (c-Hap, ICDD-PDF 00-019-0272), as suggested by the position of the peak at 32.2°, and Hap, as indicated by a strong peak at 31.8° and an additional peak at 10.8°.

In the ATR-FTIR spectra (see Fig. 1), the characteristic signals of PO_4^{3-} groups can be identified for all samples. In detail, the intense bands at 1087 and 1021 cm^{-1} , attributed to the asymmetric stretching modes of P–O, a signal at 963 cm^{-1} attributed to the symmetric stretching mode and the corresponding bending mode at 602 and 560 cm^{-1} can be singled out.²⁹ In comparison to Hap-1, samples obtained from the acid dissolution of ES powder seem to present a higher degree of

Table 1 Overview of the synthesized samples and the literature sample used for comparison in the GCM approach

Sample	Ca source	ES treatment	Composition
Hap-1	$\text{Ca}(\text{OH})_2$	—	Hap
Hap-2	ES	Dissolution in HNO_3 solution	Hap + c-Hap
Hap-3	ES	Dissolution in HAsc solution	Hap + $\text{CaOx} \cdot \text{H}_2\text{O}$ + $\text{CaOx} \cdot 2\text{H}_2\text{O}$
Hap-4 (ref. 27)	ES	Calcinated at 900 °C	c-Hap





Fig. 1 ATR-FTIR spectrum of Hap-1 (black line), Hap-2 (blue line) and Hap-3 (red line).

hydration. As evident in Fig. 1, the spectral component characteristic of free hydroxyl groups, located at 3570 cm^{-1} , is overlapped by a broad band, centred at 3400 cm^{-1} , characteristic of water molecules/OH groups interacting *via* hydrogen bonding. The corresponding bending mode of this group is observed at $1630\text{--}1640\text{ cm}^{-1}$.³⁰ Other spectral features are observed for all samples: components located at 1487 , 1405 and 873 cm^{-1} are attributable to the asymmetric stretching mode and to the out-of-plane bending mode of surface carbonate species.³¹ In the spectrum of Hap-2, some other bands are observed at 1450 and 830 cm^{-1} , indicative of a B-type substitution of PO_4^{3-} by CO_3^{2-} in the crystalline lattice of Hap.³² A peak at 1355 cm^{-1} is also evident, and can be attributed to asymmetric stretching mode of residual nitrate groups.³³ Moreover, in the spectrum of Hap-3, the characteristic spectral component of oxalate ions is observed at 1595 , 1318 and 783 cm^{-1} (C–O modes).³⁴ Other bands are also evident at 1723 and 757 cm^{-1} , and can be attributed to the presence of ascorbate-related species.³⁵ The presence of an organic fraction in Hap-3 was confirmed by TGA (see Fig. S4). Increasing the T , two weight loss steps were observed: the first in the $25\text{--}200\text{ }^\circ\text{C}$ range,

corresponding to water loss, and the second in the $300\text{--}500\text{ }^\circ\text{C}$ range, associated to the decomposition of the organic fraction.³⁶ This second step was not observed in the TGA of Hap-1.

FESEM images of Hap-1 and Hap-2 (See Fig. 2) reveal the formation of aggregated nanoparticles with average dimension below 200 nm , predominantly exhibiting a needle-like morphology, mostly elongated along a specific crystallographic direction, as expected for Hap materials. In fact, both samples present a quite large SSA, 122 and $164\text{ m}^2\text{ g}^{-1}$, respectively. The particles also appear homogeneous in both shape and size. In contrast, in the case of Hap-3, the nanoparticles are predominantly round-shaped and not only aggregated but also show a tendency to coalesce. This feature could be correlated to the co-presence of oxalate phases. These results are consistent with the low value of SSA of Hap-3 ($17\text{ m}^2\text{ g}^{-1}$).

To evaluate whether the proposed approach is advantageous and aligned with the principles of green chemistry,²⁴ the GCM approach was applied to each of the synthesized samples (Hap-1, Hap-2 and Hap-3). For comparison, the GMC approach²⁵ was applied to HAP obtained by Núñez, D. *et al.*²⁷ using a wet precipitation method analogous to our procedure, but involving the calcination step to transform ES into CaO (Hap-4). The results are detailed in Table S1. As shown in Fig. 3, the proposed approach, dissolving ES in HAsc, leads to a significant improvement in energy efficiency with respect to the process involving calcination. The higher energy efficiency compared to Hap-1 is related to the

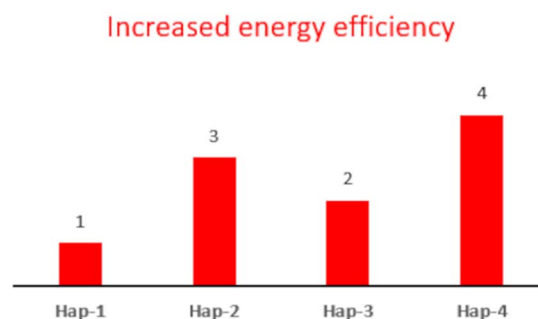


Fig. 3 Bar graph showing the category ranking of Hap samples for the category increased energy efficiency.

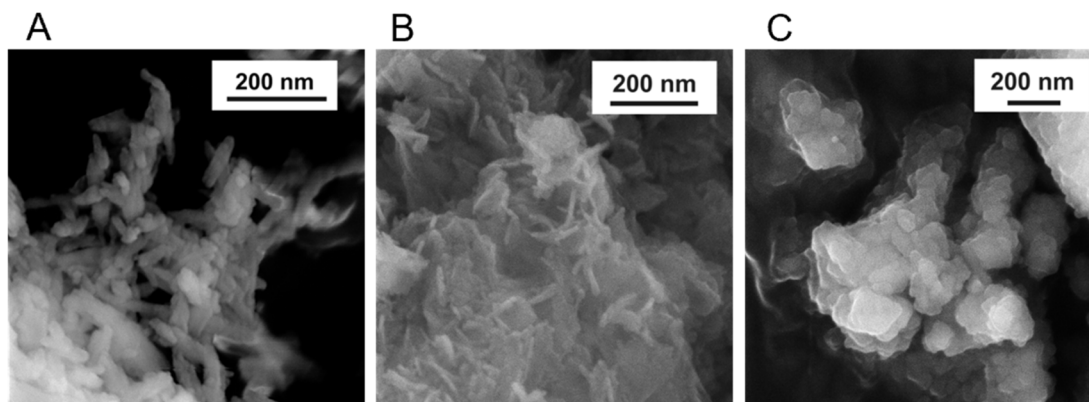


Fig. 2 SEM images of Hap-1 (A), Hap-2 (B) and Hap-3 (C) samples.





Fig. 4 Cumulative wt% of released Ca (A), P (B) and K ions (C) in water from Hap-1 (black), Hap-2 (blue) and Hap-3 (red).

presence of a supplementary synthetic step. For the reduced human and environmental hazard category, the different syntheses show comparable values, but as expected, the process involving HNO_3 presents a higher risk, involving the use of a strong acid (see Fig. S5). The results indicate that further studies are needed to improve the resource use category (see Fig. S5). A possible approach could consist in the employment of waste-derived materials. For instance, HAsc can be extracted from natural sources, as it is abundant in various fruits and vegetables such as kiwis, citrus fruits, tomatoes, and bell peppers.³⁷ Moreover, as for the basification step, the use of ashes derived from biomass combustion could be considered as a more sustainable alternative.

Ion release study

To assess the potential use of the obtained materials for soil amendments, tests were conducted to evaluate the availability of nutrients, quantifying the amount of phosphorus, calcium and potassium ions released in water (in steps of 24 h). The release profiles of Ca and P ions exhibit similar trends, releasing a constant amount in every step. In contrast, a great amount of K ions is released within the first 24 h, after which it becomes very low (see Fig. 4).

The results show that Hap samples obtained from ES release higher amounts of nutrients if compared to pure Hap (Hap-1), as shown in Table 2 (and Tables S2–S4). The results indicate that Hap-3 is the most promising candidate to be employed as a soil amendment, being capable of delivering a significant amount of nutrients. Hap-3 releases three times the amount of %wt of Ca compared to Hap-1 (pure Hap), and twice the amount compared to Hap-2. Notably, Hap-3 releases around 70 times more phosphorus by weight than Hap-1 and around three times more than Hap-2.

Table 2 Quantities of Ca, P and K released in water

Sample	Ca _{TOT} (mg)	Ca% ^a	P _{TOT} (mg)	P% ^a	K _{TOT} (mg)	K% ^a
Hap-1	0.20	0.32	0.45	1.4	0.0026	0.45
Hap-2	0.30	0.70	0.44	2.1	6.9	35
Hap-3	1.4	1.2	1.2	8.2	5.3	54

^a wt% of released ion/total.

This behaviour could be related to a locally (*i.e.*, at the surface) more acidic environment due to the presence of residual HAsc (and its derivatives) that promotes the dissolution of the particle, as suggested by previous studies.^{38,39}

Conclusions

The various physico-chemical characterization techniques demonstrated that it is possible to obtain Hap from an economical and sustainable waste product, such as ES, avoiding high T treatments. When ESs are dissolved in a strong acid, such as HNO_3 , carbonated-Hap is obtained, due to the formation of a large amount of CO_2 that is partially trapped in the solid product. This result is similar to those observed in literature studies that involved the use of strong and medium strength acids. We developed a green approach using HAsc, a non-toxic and cost-effective reagent that has a dual role: it dissolves ES and traps the formed CO_2 in the form of oxalate ions. To fulfil the circular economy perspective, we tailored the material for soil amendment applications. Furthermore, as demonstrated by the GCM approach, the elimination of the calcination step leads to a significant improvement in terms of energy efficiency. In the pursuit of a greener approach, efforts will be made to optimize the synthesis to improve resource use by increasing the proportion of reagents derived from waste products. A further perspective involves the search for sustainable sources of phosphate species.

Among the synthesized materials, the Hap-containing composite obtained by dissolution of ES with HAsc (Hap-3) was identified as a promising candidate for soil amendment applications. The presence of ascorbate-related species improves the availability of K, P and Ca nutrients, while the presence of calcium oxalate may also offer additional benefits by contributing to soil pH regulation and nutrient availability. Future studies on nutrient release in soil are necessary to assess both efficiency and applicability of Hap-3 as a solid fertilizer.

Author contributions

Methodology: A. G., G. C., and L. O.; formal analysis: L. C., A. G. and M. M.; investigation: L. C., A. G. and G. C.; conceptualization: A. G. and G. C.; writing—original draft: L. C. and A. G.;



writing—review and editing: L. O., M. M. and G. C.; supervision: L. O. and G. C.; project administration: G. C.; funding acquisition: A. G. and G. C.

Conflicts of interest

There are no conflicts to declare.

Data availability

The data supporting this article have been included as part of the supplementary information (SI). Supplementary information: experimental and characterization details; PXRD and TGA data; score for the GMC approach and ES characterization data. See DOI: <https://doi.org/10.1039/d5su00577a>.

Acknowledgements

A.G. acknowledges MUR (Ministero dell'Università e della Ricerca), PON R&I 2014-2020-Asse IV "Istruzione e Ricerca per il recupero-REACT-EU", Azione IV.6 "Contratti di Ricerca su tematiche Green".

Notes and references

- 1 B. Mishra, *et al.*, Valorization of agro-industrial biowaste to biomaterials: an innovative circular bioeconomy approach, *Circular Economy*, 2023, **2**, 100050.
- 2 FAO, Agricultural production statistics 2010–2023, *FAOSTAT Analytical Briefs*, Rome, 2024, No. 96, <https://openknowledge.fao.org/handle/20.500.14283/cd3755en>.
- 3 M. Waheed, *et al.*, Channelling eggshell waste to valuable and utilizable products: a comprehensive review, *Trends Food Sci. Technol.*, 2020, **106**, 78–90.
- 4 V. Vandeginste, Food waste eggshell valorization through development of new composites: a review, *Sustainable Mater. Technol.*, 2021, **29**, e00317.
- 5 P. Arokiasamy, *et al.*, Synthesis methods of hydroxyapatite from natural sources: a review, *Ceram. Int.*, 2022, **48**, 14959–14979.
- 6 E. Bernalte, J. Kamieniak, E. P. Randviir, Á. Bernalte-García and C. E. Banks, The preparation of hydroxyapatite from unrefined calcite residues and its application for lead removal from aqueous solutions, *RSC Adv.*, 2019, **9**, 4054–4062.
- 7 J. Carvalho, J. Araujo and F. Castro, Alternative low-cost adsorbent for water and wastewater decontamination derived from eggshell waste: an overview, *Waste Biomass Valorization*, 2011, **2**, 157–167.
- 8 K. Adaikalam, *et al.*, Eco-Friendly Facile Conversion of Waste Eggshells into CaO Nanoparticles for Environmental Applications, *Nanomaterials*, 2024, **14**, 1620.
- 9 R. B. Saldanha, C. G. Da Rocha, A. M. L. Caicedo and N. C. Consoli, Technical and environmental performance of eggshell lime for soil stabilization, *Constr. Build. Mater.*, 2021, **298**, 123648.
- 10 S. Grzeszczyk, *et al.*, Characterization of eggshell as limestone replacement and its influence on properties of modified cement, *Constr. Build. Mater.*, 2022, **319**, 126006.
- 11 A. T. Admase, T. N. Gesese, S. W. Fenta and B. G. Eshete, Synthesis and characterization of bio-based eco-friendly biofilm composites reinforced with waste eggshell powder, *Sci. Rep.*, 2025, **15**, 31617.
- 12 Z. Kareem and E. Eyiler, Synthesis of hydroxyapatite from eggshells *via* wet chemical precipitation: a review, *RSC Adv.*, 2024, **14**, 21439–21452.
- 13 M. S. Firdaus Hussin, H. Z. Abdullah, M. I. Idris and M. A. Abdul Wahap, Extraction of natural hydroxyapatite for biomedical applications—a review, *Heliyon*, 2022, **8**, e10356.
- 14 M. Lee, W.-S. Tsai and S.-T. Chen, Reusing shell waste as a soil conditioner alternative? A comparative study of eggshell and oyster shell using a life cycle assessment approach, *J. Cleaner Prod.*, 2020, **265**, 121845.
- 15 M. R. Maghsoodi, L. Ghodszad and B. Asgari Lajayer, Dilemma of hydroxyapatite nanoparticles as phosphorus fertilizer: Potentials, challenges and effects on plants, *Environ. Technol. Innovation*, 2020, **19**, 100869.
- 16 A. Fihri, C. Len, R. S. Varma and A. Solhy, Hydroxyapatite: a review of syntheses, structure and applications in heterogeneous catalysis, *Coord. Chem. Rev.*, 2017, **347**, 48–76.
- 17 A.-R. Ibrahim, W. Wei, D. Zhang, H. Wang and J. Li, Conversion of waste eggshells to mesoporous hydroxyapatite nanoparticles with high surface area, *Mater. Lett.*, 2013, **110**, 195–197.
- 18 N. Tangboriboon, J. Suttiprapar, S. Changkhamchom and A. Sirivat, Alternative green preparation of mesoporous calcium hydroxyapatite by chemical reaction of eggshell and phosphoric acid, *Int. J. Appl. Ceram. Technol.*, 2019, **16**, 1989–1997.
- 19 F. HamidiVadigh and J. Javadpour, Synthesis of Hydroxyapatite Nanoparticles Using Eggshells and Two Different Phosphate Sources, *EJENG*, 2024, **9**, 1–4.
- 20 L. Pastero, *et al.*, CO₂ capture and sequestration in stable Ca-oxalate, *via* Ca-ascorbate promoted green reaction, *Sci. Total Environ.*, 2019, **666**, 1232–1244.
- 21 P. Li, *et al.*, Oxalate in Plants: Metabolism, Function, Regulation, and Application, *J. Agric. Food Chem.*, 2022, **70**, 16037–16049.
- 22 W. C. Graustein, K. Cromack and P. Sollins, Calcium Oxalate: Occurrence in Soils and Effect on Nutrient and Geochemical Cycles, *Science*, 1977, **198**, 1252–1254.
- 23 G. Martin, *et al.*, Fungi, bacteria and soil pH: the oxalate-carbonate pathway as a model for metabolic interaction, *Environ. Microbiol.*, 2012, **14**, 2960–2970.
- 24 J. C. Warner, A. S. Cannon and K. M. Dye, Green chemistry, *Environmental Impact Assessment Review*, 2004, **24**, 775–799.
- 25 A. DeVierno Kreuder, *et al.*, A Method for Assessing Greener Alternatives between Chemical Products Following the 12 Principles of Green Chemistry, *ACS Sustainable Chem. Eng.*, 2017, **5**, 2927–2935.
- 26 V. Aina, *et al.*, Magnesium- and strontium-co-substituted hydroxyapatite: the effects of doped-ions on the structure



- and chemico-physical properties, *J. Mater. Sci.: Mater. Med.*, 2012, **23**, 2867–2879.
- 27 D. Núñez, E. Elgueta, K. Varaprasad and P. Oyarzún, Hydroxyapatite nanocrystals synthesized from calcium rich bio-wastes, *Mater. Lett.*, 2018, **230**, 64–68.
- 28 D. Núñez, E. Elgueta, K. Varaprasad and P. Oyarzún, Hydroxyapatite nanocrystals synthesized from calcium rich bio-wastes, *Mater. Lett.*, 2018, **230**, 64–68.
- 29 S. Koutsopoulos, *Synthesis and Characterization of Hydroxyapatite Crystals: A Review Study on the Analytical Methods*, 2002.
- 30 Y. Sakhno, P. Ivanchenko, M. Iafisco, A. Tampieri and G. Martra, A Step toward Control of the Surface Structure of Biomimetic Hydroxyapatite Nanoparticles: Effect of Carboxylates on the {010} P-Rich/Ca-Rich Facets Ratio, *J. Phys. Chem. C*, 2015, **119**, 5928–5937.
- 31 J. D. Termine and D. R. Lundy, Hydroxide and carbonate in rat bone mineral and its synthetic analogues, *Calc. Tis Res.*, 1973, **13**, 73–82.
- 32 F. Ren, Y. Ding and Y. Leng, Infrared spectroscopic characterization of carbonated apatite: A combined experimental and computational study, *J. Biomed. Mater. Res., Part A*, 2014, **102**, 496–505.
- 33 F. J. Carmona, *et al.*, The role of nanoparticle structure and morphology in the dissolution kinetics and nutrient release of nitrate-doped calcium phosphate nanofertilizers, *Sci. Rep.*, 2020, **10**, 12396.
- 34 V. Asyana *et al.*, Analysis of urinary stone based on a spectrum absorption FTIR-ATR. in *Analysis of urinary stone based on a spectrum absorption FTIR-ATR*, Institute of Physics Publishing, 2016, vol. 694.
- 35 C. Y. Panicker, H. T. Varghese and D. Philip, FT-Raman and SERS spectra of Vitamin C, *Spectrochim. Acta, Part A*, 2006, **65**, 802–804.
- 36 D. Hourlier, Thermal decomposition of calcium oxalate: beyond appearances, *J. Therm. Anal. Calorim.*, 2019, **136**, 2221–2229.
- 37 M. Ali Sheraz, M. Fatima Khan, S. Ahmed & S. Hafeez Kazi, *Stability and Stabilization of Ascorbic Acid*, 2015, <https://www.researchgate.net/publication/321148774>.
- 38 U. Sittitit, J. Jettanasen, S. Supothina and R. Rattanakam, Dissolution Performance of Carbon/Hydroxyapatite Nanocomposite Prepared from Fish Scales, *Inorganics*, 2022, **10**, 242.
- 39 A. Giordana, *et al.*, Biostimulants derived from organic urban wastes and biomasses: an innovative approach, *Front. Chem.*, 2023, **11**, 969865.

